

Determining the BDMPS transport coefficient via medium-modified fragmentation functions

Carlos A. Salgado and Urs Achim Wiedemann

Theory Division, CERN, CH-1211 Geneva 23, Switzerland.

In nucleus-nucleus collisions at RHIC and LHC, partons produced at high transverse momentum can undergo multiple scattering within the collision region prior to fragmenting into hadrons. We have studied the resulting medium-modified fragmentation function based on a calculation of the BDMPS-Z medium-induced gluon radiation for a dense, expanding medium of small finite extension. Here we explain how the BDMPS transport coefficient \hat{q} which measures the energy density attained in the collision, can be extracted from the observed modification of high- p_\perp hadroproduction. We also comment on the significant remaining uncertainties in extracting \hat{q} from data.

To leading order in perturbative QCD, high- p_\perp hadroproduction in proton-proton collisions is described by the factorization formula

$$\frac{d\sigma^h}{dp_t^2 dy} = K(\sqrt{s}) \int \frac{dz}{z^2} \int dy_2 \sum_{i,j} x_1 f_i^A(x_1, Q^2) x_2 f_j^B(x_2, Q^2) \frac{d\sigma^{ij \rightarrow k}}{d\hat{t}} D_{k \rightarrow h}(z, Q^2). \quad (1)$$

Here f_i^A, f_j^B are the proton parton distribution functions (PDF), $d\sigma^{ij \rightarrow k}/d\hat{t}$ is the partonic cross section and $D_{k \rightarrow h}(z, Q^2)$ describes the fragmentation of a parton k into the hadron h carrying a fraction z of the momentum. Eq. (1) leads to a fair description of the shape of high- p_\perp hadronic spectra while the normalisation has to be adjusted by an energy-dependent K -factor (see e.g. [1]). Also to NLO, the disagreement between theory and experiment lies essentially in an albeit reduced normalisation factor [2].

For nucleus-nucleus collisions, additional corrections arise due to parton density effects. At sufficiently high p_\perp where the factorised form (1) is expected to hold, two corrections are known: i) Density effects in the *initial state* can be parametrised by nuclear PDFs for which global fits are available [3]. At RHIC energies, however, this is only a small correction [1] [4]. ii) Density effects in the *final state* affect the fragmentation of the high p_\perp parton produced in the hard collision. Several studies indicate that the dominant final state correction is due to medium-induced gluon radiation and the ensuing parton energy loss. If the high p_\perp parton loses with probability $P_E(\epsilon)$ a fraction ϵ of its energy while propagating through the medium, then its medium-modified fragmentation function can be written as [5,6,7]

$$D_{k \rightarrow h}^{(\text{med})}(z, Q^2) = \int_0^1 d\epsilon P_E(\epsilon) \frac{1}{1-\epsilon} D_{k \rightarrow h}\left(\frac{z}{1-\epsilon}, Q^2\right). \quad (2)$$

We have calculated the *quenching weights* $P_E(\epsilon)$ for quarks and gluons starting from the BDMPS-Z [8,9,10,11] gluon radiation spectrum $dI/d\omega$ generalised to the case of an expanding medium of small finite size [7]. For the case of a static medium, the resulting finite size corrections to the BDMPS-expression of $dI/d\omega$ are shown in Fig. 1. They become important for gluon energies much smaller than the characteristic gluon frequency $\omega_c = \hat{q} L$. The latter depends on the in-medium path-length L and the BDMPS transport coefficient \hat{q} which measures the amount of transverse momentum squared transferred from the medium to the hard parton per unit path-length. For a static medium, the radiation spectrum depends only on ω_c and the dimensionless parameter combination $R = \frac{1}{2}\hat{q} L^3$. As seen in Fig. 1, the BDMPS case is the limit $L \rightarrow \infty$ of our calculation keeping ω_c finite.

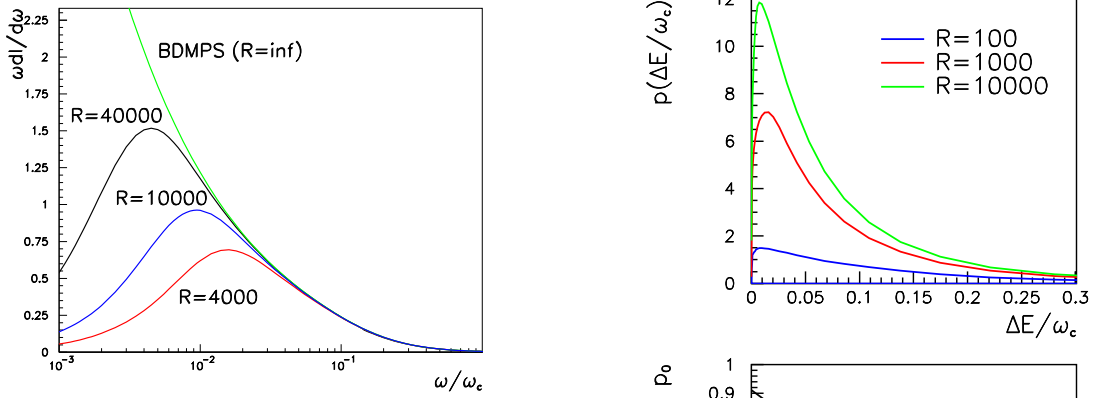


Figure 1. (Up) Gluon radiation spectrum, $\omega dI/d\omega$, for several values of R and comparison with the BDMPS result.

Figure 2. (Right) Continuous (upper figure) and discrete (lower) contributions to the quenching weight $P_E(\epsilon)$ of a fast quark for different values of R .

Quenching weights are evaluated in the independent gluon emission approximation [12] and show both a discrete and a continuous contribution (see Fig. 2),

$$P_E(\epsilon) = \sum_{n=0}^{\infty} \frac{1}{n!} \left[\prod_{i=1}^n \int d\omega_i \frac{dI(\omega_i)}{d\omega} \right] \delta \left(\epsilon - \sum_{i=1}^n \frac{\omega_i}{E} \right) \exp \left[- \int d\omega \frac{dI}{d\omega} \right] \quad (3)$$

$$= p_0 \delta(\epsilon) + p(\epsilon). \quad (4)$$

Here, $P(\epsilon)$ is a generalised probability of norm 1. For a medium of finite length L , there is a finite probability p_0 that the fragmentation is not disturbed by the medium. This discrete contribution decreases with increasing in medium path-length or increasing density of the medium.

The transport coefficient is proportional to the density of scattering centres, $\hat{q}(\tau) \propto n(\tau)$. The dynamical expansion of the collision region can be parametrised by a power

law decrease in proper time, $n(\tau) = n_0 \left(\frac{\tau_0}{\tau}\right)^\alpha$, where $\alpha = 0$ for static, $\alpha = 1$ for Bjorken expansion. Fig. 3 shows the gluon radiation spectrum for different values of α with parameters ω_c and R written in terms of the linearly weighted transport coefficient

$$\bar{q} = \frac{2}{L^2} \int_{\tau_0}^{\tau_0+L} d\tau (\tau - \tau_0) \hat{q}(\tau). \quad (5)$$

After rescaling according to (5), the radiation spectra $dI/d\omega$ calculated for different values α coincide (see Fig. 3). This establishes a dynamical scaling law [7] which simplifies calculations considerably since results for a dynamically expanding medium can be obtained by scaling the result obtained for a static medium. It extends earlier findings of dynamical scaling of the average energy loss [10,6,13] to the ω -differential radiation spectrum [7].

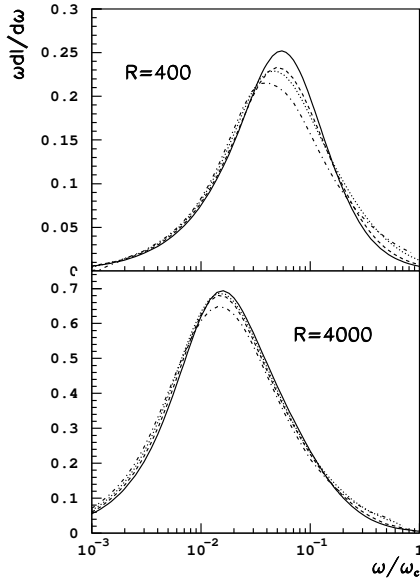


Figure 3. The gluon radiation spectrum, $\omega dI/d\omega$, plotted as a function of $\omega_c = \bar{q}L$ and $R = \frac{1}{2}\bar{q}L^3$. Different curves correspond to different expansion parameters $\alpha = 0, 0.5, 1.0$ and 1.5 .

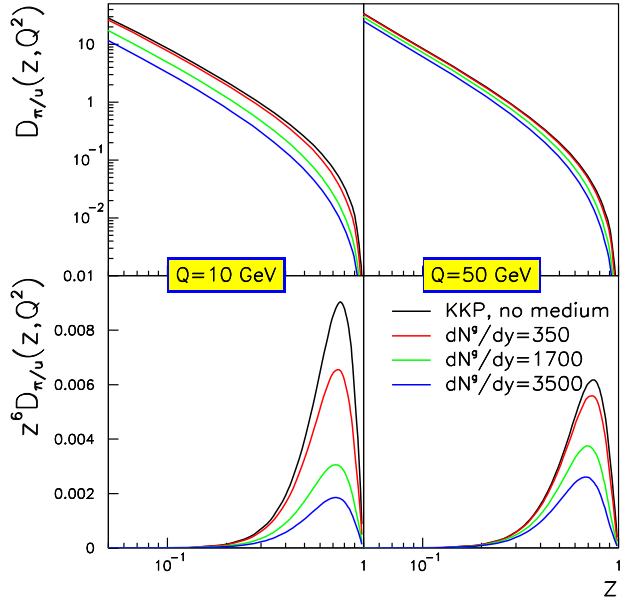


Figure 4. The LO KKP [14] fragmentation function $u \rightarrow \pi$ for no medium and the medium-modified fragmentation functions for different gluon rapidity densities in a medium of length $L = 7$ fm.

Based on the quenching weights (3) for static and expanding media, we have calculated medium-modified fragmentation functions according to (2), using the KKP parametrisation [14] for parton fragmentation in the vacuum (see Fig. 4). The virtuality Q of the parent parton is identified with its initial transverse energy. For a medium showing one-dimensional Bjorken expansion ($\alpha = 1$), the transport coefficient \bar{q} is related to the gluon rapidity density as [6,8,7]

$$R = \frac{1}{2}\bar{q}L^3 = \frac{L^2}{R_A^2} \frac{dN^g}{dy}. \quad (6)$$

The calculation presented in Fig. 4 allows to determine medium modifications to the transverse momentum spectrum (1) at sufficiently high p_\perp . While this last step is not

yet performed, one can estimate the effect based on the observation [1] that the hard partonic cross section in (1) essentially weighs the fragmentation function with the power z^6 . Inspecting the corresponding unintegrated moment $z^6 D_{\pi/u}(z, Q^2 \sim p_\perp^2)$ in Fig. 4, one estimates that a factor 2 suppression of the hadronic pion spectrum for $p_\perp \sim 6\text{--}7$ GeV corresponds to an initial gluon density of 500–1000. For an in-medium path-length of $L = 7$ fm, this amounts to a line-averaged transport coefficient $\bar{q} = (300 \text{ MeV})^2 - (600 \text{ MeV})^2/\text{fm}$ which corresponds to $\langle p_\perp^2 \rangle/L_{\text{med}}$ of several GeV^2/fm within the first two fm/c.

For a reliable determination of \hat{q} from data, the evaluation of (1) is not sufficient. One also has to discriminate the medium modification discussed here from other corrections to (1), such as “soft” hadronic contributions at low p_\perp and higher order perturbative contributions at high p_\perp . Much of this can be done by studying the dependence of spectra on the in-medium path-length e.g. via the centrality dependence of high- p_\perp hadroproduction and monojet/dijet production. Another discriminatory tool results from the fact that medium-induced gluon radiation is a medium-enhanced power correction which shows a power law decrease with increasing p_\perp . This is in contrast e.g. to perturbative NLO corrections which mainly affect the normalisation but not the shape of spectra. This will also provide an important additional cross check at LHC: according to (6), if the rapidity density increases by a factor 5 from RHIC to LHC, and if the suppression factor 2 for RHIC π^0 spectra [15] at $p_\perp \sim 6\text{--}7$ GeV can be attributed solely to medium-induced gluon radiation, then a factor 2 suppression of the corresponding spectrum at LHC is expected in the range $p_\perp \sim 40\text{--}50$ GeV. At even higher p_\perp still accessible at LHC, this suppression would decrease according to a power law, thus leading to a modified p_\perp -shape of hadronic spectra.

C.A.S. is supported by a Marie Curie Fellowship of the European Community programme TMR (Training and Mobility of Researchers), under the contract number HPMF-CT-2000-01025.

REFERENCES

1. K.J. Eskola and H. Honkanen, [arXiv:hep-ph/0205048].
2. P. Aurenche, *et al.* Eur. Phys. J. C **13** (2000) 347.
3. K. J. Eskola, V. J. Kolhinen and C. A. Salgado, Eur. Phys. J. C **9**, 61 (1999).
4. I. Sarcevic, these proceedings.
5. X. N. Wang, Z. Huang and I. Sarcevic, Phys. Rev. Lett. **77** (1996) 231.
6. M. Gyulassy, I. Vitev and X. N. Wang, Phys. Rev. Lett. **86** (2001) 2537.
7. C. A. Salgado and U. A. Wiedemann, Phys. Rev. Lett. **89** (2002) 092303.
8. R. Baier et al. Nucl. Phys. B **483** (1997) 291; Nucl. Phys. B **484** (1997) 265.
9. B. G. Zakharov, JETP Lett. **65** (1997) 615.
10. R. Baier et al. Phys. Rev. C **58** (1998) 1706.
11. U. A. Wiedemann, Nucl. Phys. B **588** (2000) 303; Nucl. Phys. A **690** (2001) 731.
12. R. Baier, Y. L. Dokshitzer, A. H. Mueller and D. Schiff, JHEP **0109** (2001) 033.
13. E. Wang and X. N. Wang, arXiv:hep-ph/0202105.
14. B. A. Kniehl, G. Kramer and B. Pötter, Nucl. Phys. B **597** (2001) 337
15. G. David [PHENIX Collaboration], Nucl. Phys. A **698** (2002) 227.